Virology 406 (2010) 21–27

Contents lists available at ScienceDirect

Virology

journal homepage: www.elsevier.com/locate/yviro

Ring structure amino acids affect the suppressor activity of *melon aphid-borne yellows virus* P0 protein

Yan-Hong Han [a,b], Hai-Ying Xiang [a,b], Qian Wang [a,b], Yuan-Yuan Li [a,b], Wen-Qi Wu [a,b], Cheng-Gui Han [a,b,*], Da-Wei Li [a], Jia-Lin Yu [a]

[a] State Key Laboratory for Agrobiotechnology, China Agricultural University, Beijing, P. R. China
[b] Agricultural Ministry Key Laboratory for Plant Pathology, China Agricultural University, Beijing, P. R. China

ARTICLE INFO

Article history:
Received 29 January 2010
Returned to author for revision 23 June 2010
Accepted 25 June 2010
Available online 27 July 2010

Keywords:
Melon aphid-borne yellows virus
RNA silencing suppressor
P0
Trp 212

ABSTRACT

Melon aphid-borne yellows virus (MABYV) is a newly identified polerovirus occurring in China. Here, we demonstrate that the MABYV encoded P0 ($P0^{MA}$) protein is a strong suppressor of post-transcriptional gene silencing (PTGS) with activity comparable to *tobacco etch virus* (TEV) HC-Pro. In addition we have shown that the LP F-box motif present at the N-terminus of $P0^{MA}$ is required for suppressor activity. Detailed mutational analyses on $P0^{MA}$ revealed that changing the conserved Trp 212 with non-ring structured amino acids altered silencing suppressor functions. Ala substitutions at positions 12 and 211 for Phe had no effect on P0 suppression-activity, whereas Arg and Glu substitutions had greatly decreased suppressor activity. Furthermore, substitutions targeting Phe at position 30 also resulted in reduced P0 suppression-activity. Altogether, these results suggest that ring structured Trp/Phe residues in P0 have important roles in suppressor activity.

Introduction

Melon aphid-borne yellows virus (MABYV) is a newly identified *Polerovirus* from China. MABYV often co-exists in plants with another member of this genus, *Cucurbit aphid-borne yellows virus* (CABYV), but little is known about the pathogenicity, serological specificity, or vector transmission of MABYV (Xiang et al., 2008). Like other *Polerovirus* members, MABYV comprises a plus sense-RNA genome encapsidated in icosahedral virions that encodes 6 ORFs. MABYV and CABYV share 51–74% sequence identity to other poleroviruses (Xiang et al., 2008). The P0 proteins encoded by an ORF from the 5'-proximal regions of the CABYV, *Turnip yellows virus* (TuYV, syn. BWYV–FL1), *Potato leaf roll virus* (PLRV) and *Sugarcane yellow leaf virus* (ScYLV) have been shown to be post-transcriptional gene silencing (PTGS) suppressors (Pfeffer et al., 2002; Mangwende et al., 2009). F-box-like domains near the amino termini of the CABYV P0 ($P0^{CA}$) and *beet western yellows virus* [BWYV P0 ($P0^{BW}$)] proteins appear to suppress PTGS by interacting with members of the SKP1-Cullin-F-box (SCF) family of E3 ubiquitin ligases (Pazhouhandeh et al., 2006), where they function in the ubiquitination, targeting, and proteosomal degradation of the Argonaute1 (AGO1) protein, a major component of RNA-induced silencing complexes (RISC) (Baumberger et al., 2007; Bortolamiol et al., 2007). A recent study indicates that the BWYV P0 protein affects RISC assembly (Csorba et al., 2010). F-box proteins are known to interact with their targets via a C-terminal leucine-rich repeat (LRR) or a WD-40 repeat domain (Cardozo and Pagano, 2004), but neither of these motifs are present in P0. However, a conserved region (K/R) IYGEDGX3FWR does exist in some polerovirus P0 proteins (Pazhouhandeh et al., 2006). Recently, Kozlowska-Makulska et al. (2009) reported that although the P0 of most BMYV (*Beet mild yellowing virus*) isolates exhibited RNA silencing suppressor activity, two BMYV isolates and six BChV (*Beet chlorosis virus*) isolates lack detectable suppressor activity. Amino acid sequence analysis of the P0 proteins of the BMYV isolates -N32 and -26 without suppressor activity failed to reveal F-box-like domain changes. In this study, we demonstrate that MABYV P0 ($P0^{MA}$) protein is a strong RNA silencing suppressor, and we have identified several potential motifs that are important for PTGS suppression.

Results

The MABYV P0 protein is a strong RNA silencing suppressor

The CABYV, TuYV, PLRV and ScYLV P0 proteins have previously been shown to be RNA silencing suppressors (Pfeffer et al., 2002; Mangwende et al., 2009). In the current study, we investigated the P0

* Corresponding author. Department of Plant Pathology, China Agricultural University, Beijing 100193, P. R. China. Fax: +86 10 62732012.
E-mail addresses: han.037@163.com (Y.-H. Han), xhy236@yahoo.com.cn (H.-Y. Xiang), Wangqian_2000zb@163.com (Q. Wang), hunan_lyy@163.com (Y.-Y. Li), commanderwolf@163.com (W.-Q. Wu), Hanchenggui@cau.edu.cn (C.-G. Han), lidw@cau.edu.cn (D.-W. Li), bnyvv@public.bta.net.cn (J.-L. Yu).

0042-6822/$ – see front matter © 2010 Elsevier Inc. All rights reserved.
doi:10.1016/j.virol.2010.06.045

proteins of Chinese isolates of MABYV, CABYV-CHN, BWYV, TuYV, and ScYLV and compared these with the CABYV type strain P0 protein, which was generously provided by Véronique Ziegler-Graff. An *Agrobacterium*-mediated infiltration system was employed to transiently co-express multiple proteins. In this system, an *Agrobacterium* strain harboring a GFP expressing plasmid, pBinGFP, was mixed with another strain carrying either a test or a control construct and the mixture was co-infiltrated into leaves of *Nicotiana benthamiana* WT or the *N. benthamiana* 16c line, designed for GFP silencing studies (Ruiz et al., 1998). The empty vector and a construct expressing the *Tobacco etch virus* (TEV) HC-Pro were used as negative and positive controls, respectively. Each of the P0 ($P0^{MA}$, $P0^{CAC}$, $P0^{BW}$, $P0^{TuY}$, $P0^{Sc}$ and $P0^{CA}$) proteins suppressed GFP silencing in leaves co-infiltrated with bacteria harboring pBinGFP (Fig. 1). In leaf sections co-infiltrated with pBinGFP and the control plasmid pBin219, the fluorescence intensity peaked at 3 days post-infiltration (dpi), and then declined rapidly over the next 2 days (Fig. 1a, panel 1). In contrast by 10 dpi, fluorescence in regions co-infiltrated with pBinGFP and $pBinP0^{MA}$, $pBinP0^{CAC}$ or $pBinP0^{TuY}$ was much higher (Fig. 1a, panels 3, 4 and 6) than areas co-infiltrated with pBinGFP and $pBinP0^{BW}$, $pBinP0^{Sc}$, $pBinP0^{CA}$ or the positive control $HC\text{-}Pro^{TEV}$ (Fig. 1a, panels 5, 7, 8 and 2). As a quantitative measure, Northern and Western blot analyses confirmed the visual observations, because the levels of GFP mRNA (Fig. 1b) or protein (Fig. 1c) extracted from sectors co-infiltrated pBinGFP with $pBinP0^{MA}$, $pBinP0^{CAC}$ or $pBinP0^{TuY}$ (Fig. 1b and c, lanes 3, 4 and 6) accumulated to a higher abundance than the pBinGFP with $pBinP0^{BW}$, $pBinP0^{Sc}$, $pBinP0^{CA}$ or $pBinHCPro^{TEV}$ co-infiltrations (Fig. 1b and c, lanes 5, 7, 8 and 2). In an additional reinforcement of the silencing suppression effectiveness of the $P0^{MA}$ protein, GFP fluorescence was apparent even at 30 dpi in co-infiltrated areas and with the longest GFP fluorescence persisting for 45 dpi, shortly before the infiltrated leaves died (Data not shown).

Phe 211 and Trp 212 mutations affect $P0^{MA}$ suppressor activity

To identify residues contributing to P0 silencing suppression, we conducted amino acid sequence alignments of nine poleroviruses and found a conserved sequence (Fig. 2), that agrees with those noted in a previous report (Pazhouhandeh et al., 2006). The PLRV and ScYLV P0 proteins have been shown to be weaker suppressors than the CABYV P0 protein (Pfeffer et al., 2002; Mangwende et al., 2009). In contrast, the BChV P0 protein appeared to have no suppressor activity in similar assays (Kozlowska-Makulska et al., 2009). A natural P0 variant of MABYV with an amino acid point mutation at position 212 also lacks suppressor activity. For these reasons, we first emphasized the C-terminal Trp 212 residue and conducted a series of substitutions targeting Trp 212 to assess the effects of the mutations on $P0^{MA}$ functions. The W212R, W212A, W212G, W212E, W212F, W212H, and W212Y substitutions were used in co-infiltration experiments, along the negative controls pBinGFP and $pBinP0^{MA}$-Stop, which contained a stop codon prior to position 43. We also included $pBinP0^{MA}$-LP(55-56) AA as a control and confirmed that the LP residues are essential for $P0^{MA}$ activity, which was expected as this sequence has been reported to be a core component of the F-box domain (Pazhouhandeh et al., 2006). At 5 dpi, GFP intensities in leaves co-infiltrated with pBinGFP and $pBinP0^{MA}$-Stop, $pBinP0^{MA}$-LP(55-56)AA, $pBinP0^{MA}$-W212R, $pBinP0^{MA}$-W212G or $pBinP0^{MA}$-W212E (Fig. 3a, panels 4, 5, 6, 8, 9) were substantially lower than in co-infiltrations with pBinGFP and wild type $pBinP0^{MA}$ (Fig. 3a, panel 3). However, leaves infiltrated with pBinGFP and $pBinP0^{MA}$-W212A exhibited an intermediate level of GFP

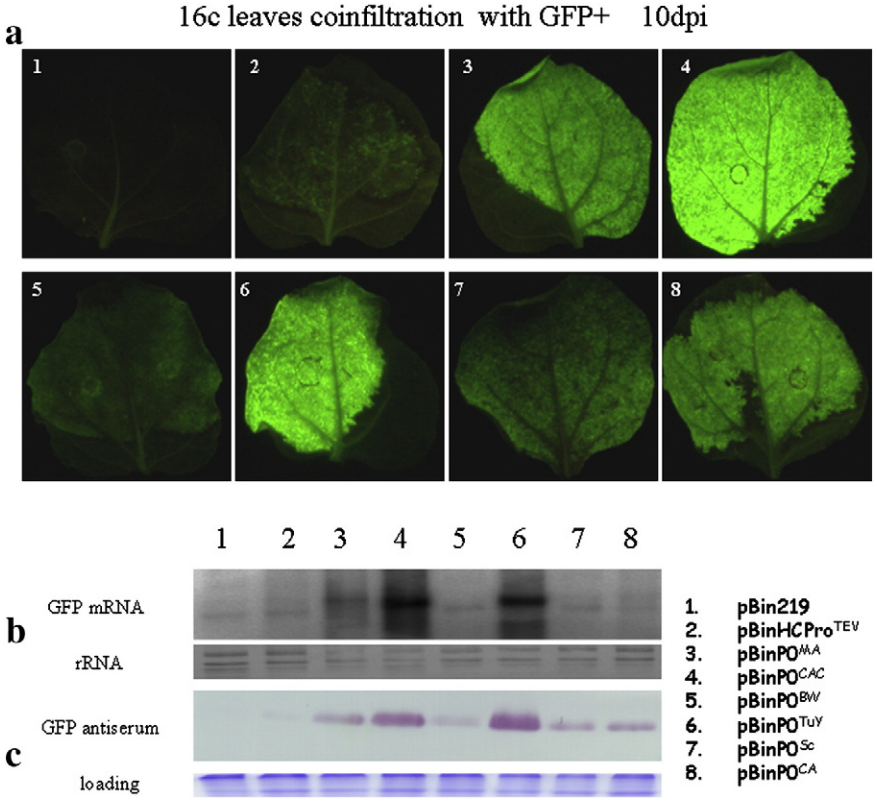

Fig. 1. Comparison of GFP PTGS suppression by the P0 proteins of MABYV, CABYV-CHN, BWYV, TuYV, ScYLV and CABYV in *N. benthamiana*. (a) Leaves of *N. benthamiana* were agro-infiltrated with pBinGFP, plus one of the following plasmids: empty vector pBin219 (panel 1), $pBinHCPro^{TEV}$ (panel 2), $pBinP0^{MA}$ (panel 3), $pBinP0^{CAC}$ (panel 4), $pBinP0^{BW}$ (panel 5), $pBinP0^{TuY}$ (panel 6), $pBinP0^{Sc}$ (panel 7), $pBinP0^{CA}$ (panel 8). Photographs were taken under a long-wavelength UV light at 10dpi. (b) Northern blot analysis of high-molecular-weight RNA extracted from the agro-infiltrated regions of 16c leaves. Blots were hybridized with probes specific for GFP mRNA and the ethidium bromide-stained 28S rRNAs were used as RNA loading controls. (c) Western blot analysis using GFP polyclonal antiserum; total proteins were extracted from the agro-infiltrated regions. Coomassie blue stained total proteins used as loading controls. The numbers of the lanes showed in panels b and c were consistent with those in panel a.

Fig. 2. Alignments of the P0 sequences of several poleroviruses. The amino acid sequences were aligned using the BioEdit program and the conserved regions are shown (GenBank accession numbers NC_010809 (MABYV), EU000535 (CABYV-CHN), X76931 (CABYV), NC_002766 (BChV), NC_003491 (BMYV-F), NC_004756 (BWYV-USA), NC_001747(PLRV), NC_000874 (ScYLV) and NC_003743 (TuYV)).

fluorescence (Fig. 3a, panel 7). In contrast, GFP fluorescence in leaves co-infiltrated with combinations of pBinGFP and pBinP0^{MA}-W212F, pBinP0^{MA}-W212H or pBinP0^{MA}-W212Y (Fig. 3a, panels 10–12) were similar to or slightly higher than those in leaves co-infiltrated with pBinGFP and wild type pBinP0^{MA}. Northern blot analysis of mRNA extracted from regions co-infiltrated with pBinGFP along with empty vector (Fig. 3b, lane 1), pBinP0^{MA}-Stop, pBinP0^{MA}-LP(55-56)AA, pBinP0^{MA}-W212R, pBinP0^{MA}-W212G or pBinP0^{MA}-W212E (Fig. 3b, lanes 4–9) had markedly lower levels of GFP mRNA accumulation than extracts from leaves that had received pBinGFP and pBinP0^{MA}-W212F, pBinP0^{MA}-W212H or pBinP0^{MA}-W212Y combinations (Fig. 3b, lanes 10–12). The levels of GFP mRNA in the latter three mutants were also equivalent to co-infiltrations with the pBinHCPro^{TEV} or pBinP0^{MA} positive controls (Fig. 3b, lanes 2 and 3). In contrast, we observed elevated levels of P0 mRNA from leaves co-infiltrated with pBinGFP and pBinP0^{MA}, pBinP0^{MA}-W212F, pBinP0^{MA}-W212H and pBinP0^{MA}-W212Y (Fig. 3c, lanes 3 and 10–12). These results show that those mutants that failed to suppress GFP silencing were also unable to suppress their own down regulation.

Because the presence of siRNAs is indicative of RNA silencing (Hamilton and Baulcombe, 1999), we carried out Northern blot hybridization to examine the accumulation of siRNAs specific for GFP mRNA (Fig. 3d). The results clearly revealed the presence of 21–24 nt siRNAs in control leaves co-infiltrated with pBinGFP and the pBin219 empty vector (Fig. 3d, lane 1), and equal or greater amounts of siRNAs were present in leaves co-infiltrated with pBinGFP and pBinP0^{MA}-Stop, pBinP0^{MA}-LP(55-56)AA, pBinP0^{MA}-W212R, pBinP0^{MA}-W212G or pBinP0^{MA}-W212E (Fig. 3d, lanes 4, 5, 6, 8 and 9). However, siRNAs were not easily detected in leaves co-infiltrated with pBinGFP in combinations with pBinHCPro^{TEV}, pBinP0^{MA}, or the mutants pBinP0^{MA}-W212F, pBinP0^{MA}-W212H and pBinP0^{MA}-W212Y (Fig. 3d, lanes 2, 3 and 10–12). An intermediate level of GFP-siRNA was observed in leaves co-infiltrated with pBinGFP and pBinP0^{MA}-W212A (Fig. 3d, panel 7). Furthermore, Western blot analysis for GFP protein confirmed the results of the GFP fluorescence images shown in Fig. 3a. The levels of GFP protein accumulating in leaves co-infiltrated with pBinGFP and either pBinP0^{MA}-W212F, pBinP0^{MA}-W212H, or pBinP0^{MA}-W212Y (Fig. 3e, lanes 10–12) appeared to be moderately higher than those of the pBinHCPro^{TEV} and pBinP0^{MA} co-infiltrations (Fig. 3e, lanes 2 and 3). In contrast, reductions in GFP protein levels were observed in leaves co-infiltrated with combinations of pBinGFP and pBinP0^{MA}-Stop, pBinP0^{MA}-LP(55-56)AA, pBinP0^{MA}-W212R, pBinP0^{MA}-W212A, pBinP0^{MA}-W212G or pBinP0^{MA}-W212E (Fig. 3e, lanes 4–9). These results show that P0^{MA} maintains its function when aromatic amino acids substituted W212 and that the related histidine imidizole side chain also is functional. However, replacement of W212 with aspartate, glutamate and alanine residues having an aliphatic alanine R group, or a glycine residue destroys P0^{MA} suppression activities. The G residue substitution lacking a side chain is neutral and nonpolar, whereas the R and E mutations are polar and elicit localized charge changes.

In order to determine whether the aromatic F211 residue preceding W212 is required for silencing, the amino acid substitutions, F211W, F211A, F211R and F211E were incorporated into P0^{MA}. In these experiments, the pBinP0^{MA}-F211W and pBinP0^{MA}-F211A mutations (Fig. 3, panels 13 and 14) retained strong suppression activity, comparable to that of wt pBinP0^{MA}. However, substitution mutants with basic, pBinP0^{MA}-F211R, or acidic, pBinP0^{MA}-F211E, residues at position 211 failed to suppress GFP silencing (Fig. 3, panels 15 and 16). To investigate whether double mutations at positions F211 and W212 had different effects, pBinP0^{MA}-FW(211-212)AA, pBinP0^{MA}- FW(211-212)RR and pBinP0^{MA}-FW(211-212)EE mutants were generated, but each of these failed to suppress GFP silencing (Fig. 3, panels 17–19). In sum, our mutant array analyses reveal that differences in the activities of various mutants depend primarily on the amino acid side chain chemistry at position 212, but that position 211 has a minor effect on silencing suppression, whereas double mutations at both positions had more dramatic effects than single amino acid changes.

Mutations of Phe residues at positions 12 and 30 also affect P0^{MA} suppressor activity

To further investigate our hypothesis that ring-like structure amino acids with aromatic, indole or imidazole side chains may affect P0^{MA} suppressor activity, we carried out more extensive P0 amino acid alignments and these revealed two N-terminal Phe residues at positions 12 and 30 (Fig. 4). To evaluate the significance of these Phe residues, we engineered two P0^{MA} non-charged alanine mutants, F12A and FL(30-31)AA, and four charged P0^{MA} mutants, F12R, FL(30-31)RA, and F12E, and FL(30-31)EA. At 5 dpi, leaves co-infiltrated with pBinGFP and pBinP0^{MA}-F12A (Fig. 5a, panel 20) had almost the same GFP intensities as those of pBinHCPro^{TEV} and pBinP0^{MA} (Fig. 3a, panels 2 and 3). In contrast, leaves co-infiltrated with pBinP0^{MA}-F12R and pBinP0^{MA}-F12E failed to suppress GFP silencing and the limited amount of GFP expression was primarily restricted to leaf veins (Fig. 5a, panels 21 and 22). Similar results were observed with the remaining double mutants at positions 30 and 31 (Fig. 5a, panels 23–25). Leaves co-infiltrated with pBinGFP and pBinP0^{MA}-FL(30-31)AA exhibited much lower GFP fluorescence and most of this was restricted to the vascular system (Fig. 5a, panel 23). In addition, the 21–24 nt GFP-specific siRNAs were easily detected by Northern blots from leaves co-infiltrated with pBinGFP and pBinP0^{MA}-FL(30-31)AA (Fig. 5d, lane 23), but were difficult to detect in extracts of leaves co-infiltrated with pBinGFP and pBinP0^{MA}-F12A (Fig. 5d, lane 20) compared to pBinHCPro^{TEV} or pBinP0^{MA} (Fig. 3d, lanes 2 and 3). GFP protein accumulation as assessed by Western blots (Fig. 5e) was similar to the amounts expected from the GFP fluorescence results shown in Fig. 5a. Taken together, these results suggest that the two conserved Phe residues at positions 12 and 30 have important roles in the ability of P0^{MA} to suppress GFP gene silencing and that only the Ala substitution maintained activity.

Discussion

The P0 proteins of several Poleroviruses serve as RNA silencing suppressors. Our current results with MABYV P0^{MA} and those of others with CABYV P0 (P0^{CA}), BWYV P0 (P0^{BW}), TuYV P0 (P0^{TuY}), PLRV P0 (P0^{PL}), ScYLV P0 (P0^{Sc}) and BMYV P0 (P0^{BM}) have implicated the P0 protein in suppression of gene silencing (Kozlowska-Makulska et al., 2009; Mangwende et al., 2009; Pfeffer et al., 2002). These active P0 proteins appear to suppress PTGS by destabilizing AGO1 protein (Baumberger et al., 2007; Bortolamiol et al., 2007), and the F-box-like domain at the N-terminal region of the protein has been shown to be important for this activity (Pazhouhandeh et al., 2006). However, in the case of the European

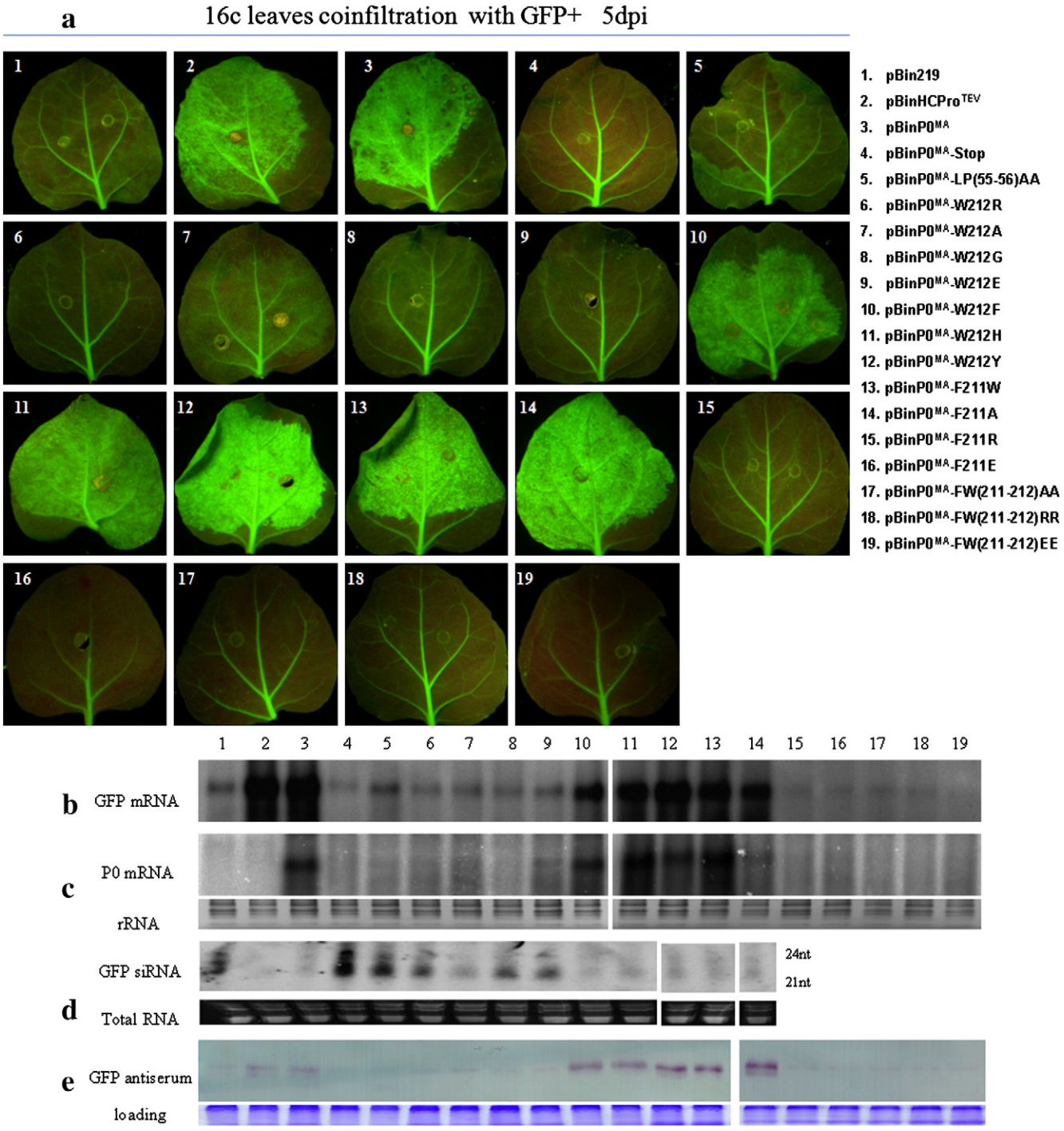

Fig. 3. PTGS suppression of GFP by P0^{MA} mutants in the *N. benthamiana* transient co-expression system. (a) Agro-infiltration of *N. benthamiana* line 16c with pBinGFP and pBin219 (panel 1), pBinHCPro^{TEV} (panel 2), pBinP0^{MA} (panel 3), pBinP0^{MA}-Stop (panel 4), pBinP0^{MA}-LP(55-56)AA (panel 5), pBinP0^{MA}-W212R (panel 6), pBinP0^{MA}-W212A (panel 7), pBinP0^{MA}-W212G (panel 8), pBinP0^{MA}-W212E (panel 9), pBinP0^{MA}-W212F (panel 10), pBinP0^{MA}-W212H (panel 11), pBinP0^{MA}-W212Y (panel 12), pBinP0^{MA}-F211W (panel 13), pBinP0^{MA}-F211A (panel 14), pBinP0^{MA}-F211R (panel 15), pBinP0^{MA}-F211E (panel 16), pBinP0^{MA}-FW(211-212)AA (panel 17), pBinP0^{MA}-FW(211-212)RR (panel 18), and pBinP0^{MA}-FW(211-212)EE (panel 19). Photographs were taken under long-wavelength UV light at 5dpi. (b and c) Northern blot analysis of high-molecular-weight RNA extracted from the agro-infiltrated regions of 16c leaves. The blots were hybridized with probes specific for (b) GFP mRNA and (c) P0 mRNA. Ethidium bromide-stained 28S rRNA was used as an RNA loading control. (d) Northern blot analysis of siRNA hybridized with an α-^{32}P UTP-radiolabeled GFP probe. Ethidium bromide-stained tRNA was used as an RNA loading control. (e) Western blot analysis using GFP polyclonal antiserum. Total proteins were extracted from agro-infiltrated regions and the numbering of the lanes are consistent to those in (a). Coomassie blue stained total proteins were used as the loading control.

isolate of BChV, the P0 protein (P0^{BC}) does not function in suppression, and the encoded P0 protein may have evolved by a recombination event with another virus (Kozlowska-Makulska et al., 2009). In this regard, P0^{BC} contains an N-terminal F-box-like domain, but diverges at the C-terminal region (Kozlowska-Makulska et al., 2009). Our work establishes that several other motif-like domains are indeed necessary for the suppressor activity of P0 protein besides F-box-like domain.

In this study we have shown that P0 proteins from different viruses (P0^{MA}, P0^{CAC}, P0^{TuY} P0^{BW}, and P0^{Sc} isolated from China) have RNA silencing suppressor activity, and among these P0^{MA}, P0^{CAC} and P0^{TuY} are stronger local PTGS suppressors than other

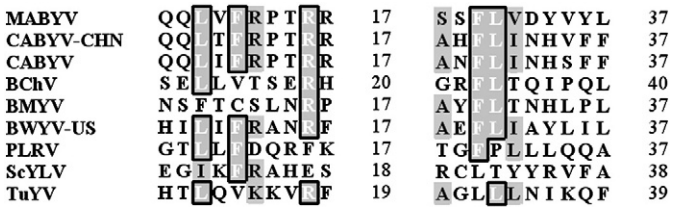

Fig. 4. Additional conserved components of polerovirus P0 proteins. Sequences were aligned by using BioEdit (GenBank accession numbers are identical to those in Fig. 2).

tested P0 proteins or TEV HC-Pro. Surprisingly, the suppression induced by $P0^{MA}$ lasted up to 45 dpi until leaves expressing $P0^{MA}$ died naturally. This contrasts generally with other P0 proteins which exhibit GFP fluorescence for up to 3 weeks, and are similar to the P0s of most BMYV isolates (Kozlowska-Makulska et al., 2009). This observation suggests that the $P0^{MA}$, $P0^{CAC}$ and $P0^{TuY}$ proteins are either more efficient suppressors of silencing or are more stable than HC-Pro in plants.

Using a battery of amino acid substitutions we have identified a single amino acid at position 212 and demonstrated that substitutions at this position can produce mutants with variable RNA silencing suppression activities. Altogether seven amino acid substitutions for Trp 212 (W212R, W212A, W212G, W212E, W212F, W212H, and W212Y), four substitutions for Phe 211 (F211W, F211A, F211R and F211E) and three double mutations for F211 and W212 [FW(211-212) AA, FW(211-212)RR and FW(211-212)EE] were evaluated for their suppressor activity. Five of the mutations (W212F, W212H, W212Y, F211W and F211A) maintained GFP expression whereas the remaining substitution mutants failed to function as silencing suppressors (Fig. 3a). These results clearly indicate that Trp 212 plays a critical role in the silencing suppression function of P0 protein, and suggest that W212 functions in concert with F211 for maximum silencing efficiency.

Protein–protein interactions are very important for biological functions and Trp and Phe are two of the most conserved amino acids found within protein hot spot sites (Ma et al., 2003; Ma and Nussinov, 2007). However, Phe-Trp substitutions normally elicit only minor differences in protein structure and biological functions (Welfle et al., 1993). The W212F and F211W mutants resulted in similar PTGS inhibition, as revealed by GFP expression and siRNA blot assays. In addition, some of the Ala substitution mutants, for example F12A, F211A and W212A, retained suppressor activity, whereas analogous Arg or Glu substitutions inactivated the P0 suppressor function. The activity of the Ala substitutions may be due to the fact that Trp to Ala normally do not disturb quaternary structure nor hydrodynamic volume of proteins, although they may alter thermal stabilities of mutant proteins (Wallace et al., 2000). Consistent with previous work, substitutions at Phe 12, Phe 211 and Trp 212 might involve via similar mechanisms to maintain the suppressor activity of $P0^{MA}$.

The reduced suppressor efficiency of the $P0^{PLRV}$ (Pfeffer et al., 2002) may be due to a FW to FR polymorphism at position 212 (Fig. 2). The fact that the P0 proteins of BChV strains lack suppressor activities (Kozlowska-Makulska et al., 2009), maybe a consequence of the absence of the FW motif (Fig. 2). Very little information is available to interpret the consequences of His or Tyr replacements of Trp residues on P0 protein structure or function; however, it is plausible that the structure of the mutant proteins is critical to changes in observed suppressor activity. In conclusion, the crystal structure of P0 is needed to elucidate the exact roles of these amino acids and/or their position in affecting their RNA silencing suppression function.

Materials and methods

Plants and plasmids

WT and GFP transgenic *N. benthamiana* line 16c plants (generously provided by Dr. David Baulcombe) were grown at 24 ± 1 °C under a 16 h light and 8 h dark regimen. The binary plasmid pBin219 was constructed by inserting the CaMV 35 S promoter into pBin19 before the multiple cloning site and was used in *N. benthamiana* leaf infiltration experiments with

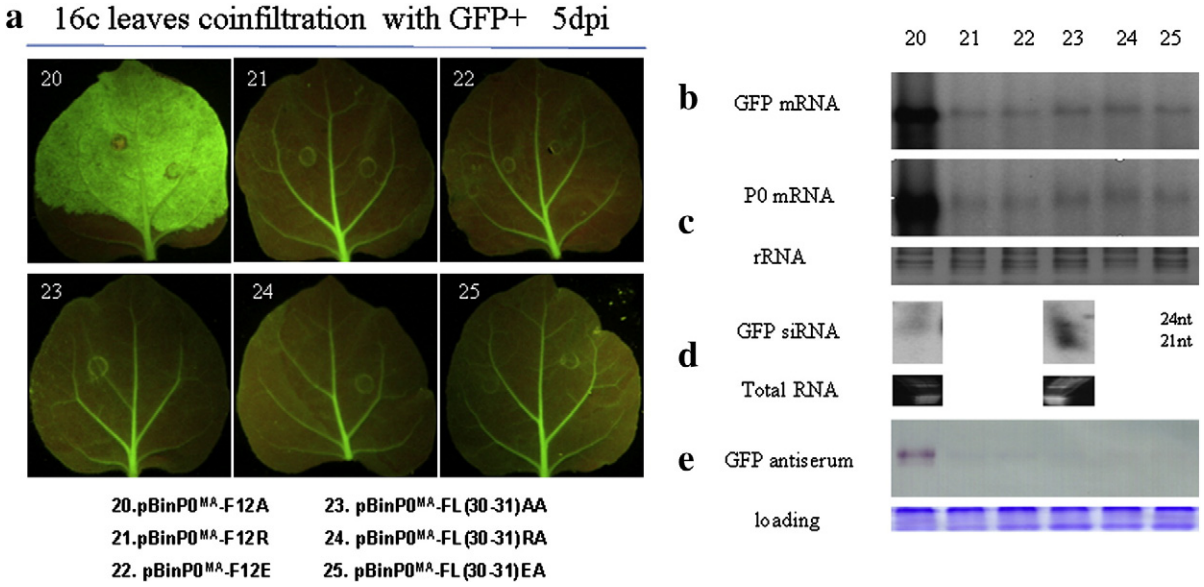

Fig. 5. PTGS suppression of GFP by $P0^{MA}$ mutants in the *N. benthamiana* transient co-expression system. (a) Agro-infiltration of *N. benthamiana* line 16c with pBinGFP and pBinP0^{MA}-F12A (panel 20), pBinP0^{MA}-F12R (panel 21), pBinP0^{MA}-F12E (panel 22), pBinP0^{MA}-FL(30-31)AA (panel 23), pBinP0^{MA}-FL(30-31)RA (panel 24), and pBinP0^{MA}-FL(30-31)EA (panel 25). Photographs were taken under long-wavelength UV light at 5dpi. (b and c) Northern blot analysis of high-molecular-weight RNA extracted from agro-infiltrated regions of 16c leaves. Blots were hybridized with probes specific for (b) GFP mRNA and (c) P0 mRNA. Ethidium bromide-stained 28S rRNA was used as an RNA loading control. (d) Northern blot analysis of siRNA hybridized with an α-^{32}P UTP-radiolabeled GFP probe. Ethidium bromide-stained tRNA was used as an RNA loading control. (e) Western blot analysis using GFP polyclonal antiserum. Total proteins were extracted from agro-infiltrated regions and the numbering of the lanes is consistent to those in (a). Coomassie blue stained total proteins were used as loading controls.

Table 1
Oligonucleotide primers used for PCR.

Primer designation	Primer sequence
MAB001F	5′- CGGGATCCACAAAAGATACAAGCGGGGGATG-3′
MAK746R	5′- GGGGTACCTCAGCTTTGTAATTCCCTTTGAAC-3′
CAB001F	5′- CGGGATCCACAAAAGATACGAGCGGGTGATG-3′
CAK740R	5′- GGGGTACCTCAGCGTTGTAAGATCTTCTGAAC-3′
BWB001F	5′- CGGGATCCACAAAAGAATATAGCGAGAAAC-3′
BWK745R	5′- GGGGTACCTCACATTTGTAAGGTCTTCTG-3′
TuB001F	5′- CGGGATCCACAAAAGAAACCAGGAGGGAATC-3′
TuB781R	5′- CGGGATCCTCATACAAACATTTCGGT-3′
MASt43F	5′- AACTTTCTACGCCTTTTTCTTG-3′
MASt43R	5′- TTCACCTTATTACCTTGTAAATTG-3′
MALP56AAF	5′- TCAGTGAGCAGCTATCAGGGGAC-3′
MALP56AAR	5′- TGAGCAGAGCCGCGCGAGCAAG-3′
MAW212RF	5′- TGCCAATTTTCCTTCTAAAAGC-3′
MAW212RR	5′- AGTCGCCTAAAATCCAAGCCG-3′
MAW212AR	5′- AGTCGCGCAAAATCCAAGCCG-3′
MAW212GR	5′- AGTCGCCCAAAATCCAAGCCG -3′
MAW212ER	5′- AGTCGTTCAAAATCCAAGCCG-3′
MAW212FR	5′- AGTCGGAAAAAATCCAAGCCG-3′
MAW212HR	5′- AGTCGATGAAAATCCAAGCCGC-3′
MAW212YR	5′- AGTCGATAAAAATCCAAGCCGCC-3′
MAF211WR	5′- AGTCGCCACCAATCCAAGCCG -3′
MAF211AR	5′-AGTCGCCAAGCATCCAAGCCGCC -3′
MAF211RR	5′- AGTCGCCACCTATCCAAGCCG-3′
MAF211ER	5′-AGTCGCCACTCATCCAAGCCG -3′
MAFW212AAR	5′-AGTCGAGCAGCATCCAAGCCGCC-3′
MAFW212RR	5′-AGTCGCCTCCTATCCAAGCCG-3′
MAFW212EER	5′-AGTCGCTCCTCATCCAAGCCG -3′
MAFL30AAF	5′-ATTACGTCTATTTGTATCAATTTAC-3′
MAFL31AAR	5′-CGACTGCAGCTGAAGATATTGAC-3′
MAFL31RAR	5′-CGACTGCCCTTGAAGATATTGAC -3′
MAFL31EAR	5′-CGACTGCCTCTGAAGATATTGAC -3′
MAF12F	5′- CAACCCGCCGAGCAAGCAC-3′
MAF12R	5′- GTCTGGCAACAAGTTGTTGTTTTAC-3′
MAF12RR	5′-GTCTCCTAACAAGTTGTTGTTTTAC-3′
MAF12ER	5′-GTCTCTCAACAAGTTGTTGTTTTAC-3′

Agrobacterium tumefaciens as a negative control. The mGFP5 gene was incorporated into pBin219 to construct pBinGFP, and the HC-Pro gene from TEV was amplified and used to generate pBinHCPro^{TEV} as a positive control. P0 proteins used in these experiments were PCR amplified from MABYV, CABYV-CHN (Xiang et al., 2008), BWYV (Han, 2008), TuYV (Xiang et al., 2009) and ScYLV (Zhou et al., 2006) cDNAs using appropriate specific primers (Table 1) (GenBank accession numbers EU000534/NC_010809, EU000535, EU636991, FJ606451 and NC_000874). A nonviral *Bam*HI restriction site was added at the 5' extremity of each forward primer, and a *Kpn*I restriction site was incorporated into each reverse primer. The *Bam*HI and *Kpn*I digested PCR fragment was ligated into *Bam*HI and *Kpn*I digested pBin219 to yield the pBinP0^{MA}, pBinP0^{CAC}, pBinP0^{BW}, pBinP0^{TuY}, pBinP0^{Sc} agro-infiltration vectors. All mutants were produced by reverse PCR using specific primers (Table 1) before inserting into *Bam*HI and *Kpn*I digested pBin219. All plasmids described above were characterized by restriction site analysis, and all the regions generated by PCR were completely sequenced.

Agro-infiltration and GFP imaging

A. tumefaciens GV3101, a gift from Dr. David Baulcombe, was transformed with each plasmid using a freeze–thaw method (Hofgen and Willmitzer, 1988). Co-infiltrations were conducted according to Voinnet et al., (1998), and each *A. tumefaciens* culture was grown to $OD_{600} \approx 1$ and mixed in equal volumes prior to infiltration. Plants were illuminated with a 100 W hand-held long-wave ultraviolet lamp (UV products, Upland, CA 91786, Black Ray model B 100AP/R) for photography and images were taken with a Nikon 4500 digital camera.

SDS-PAGE and Western blot analyses

Leaf material was ground to powder in liquid nitrogen and mixed with 2× SDS loading buffer containing 100 mM dithiothreitol (DTT), boiled at 100 °C for 5 min and clarified. Proteins were separated by 12.5% SDS-PAGE in a mini-PROTEAN 3 Cell (Bio-Rad), and transferred to Hybond-C membranes (Amersham Biosciences, Trans-Blot, Bio-Rad). The membranes were blocked overnight at 4 °C in blocking buffer (TBST (10 mmol/L Tris–HCl (pH 8.0), 150 mmol/L NaCl, 0.05% Tween-20) containing 5% non-fat milk), and incubated with 1:1000 diluted anti-GFP in blocking buffer for 2 h at 37 °C. After washing three times with TBST, the membrane was incubated with 1:5000 diluted Protein A- alkaline phosphatase (Sigma) in TBST. Finally, the GFP was detected with BCIP/NBT substrate.

Northern blotting

Total RNA from Agrobacterium-infiltrated *N. benthamiana* line 16c leaves was isolated using Trizol reagent (Invitrogen) according to the manufacturer's protocol. For Northern blot analysis of high-molecular-weight RNA, 5 μg of total RNA extracted from infiltrated leaves was separated on 1% agarose gels, transferred to Hybond-N+ membranes, and hybridized with α -^{32}PdCTP-radiolabelled GFP or P0 probes which were prepared according to the instructions accompanying the Prime-a-Gene® Labeling System (Promega). For detection of small RNAs, 50 μg of total RNA was separated on 15% polyacrylamide -7 M urea gels containing 0.5× TBE and transferred onto Hybond-N+ membranes. GFP transcript probes were radiolabeled with α-^{32}PUTP, digested with DNaseI (RNase free) for 30 min to eliminate the DNA template. The ^{32}P-labelled probes were partially hydrolyzed in sodium carbonate buffer (120 mM Na_2CO_3; 80 mM $NaHCO_3$) at 60 °C for 3 h and neutralized with 3 M sodium acetate (pH 5.2) before use. Membranes were pre-hybridized in PERFECTHYB™ (Sigma Inc.) for 1–3 h at 40 °C. After addition of the RNA probe, hybridization was performed at 38 °C overnight. The membranes were then washed four times for 10 min at 50 °C and exposed to X-ray film (Kodak X-OMAT BT Film/XBT-1).

Acknowledgments

We thank Prof Andrew O. Jackson (Department of Plant and Microbial Biology, University of California, Berkeley) for editing the manuscript and to Dr. Vanitha Ramachandran and Dr. Zhihuan Gao (Department of Plant pathology and Microbiology, University of California at Riverside) for their valuable advices. We also thank Dr. David Baulcombe for providing WT and GFP transgenic *N. benthamiana* line 16c and GV3101 and Véronique Ziegler-Graff (Institut de Biologie Moléculaire des Plantes du CNRS et de l'Université Louis Pasteur, 67084 Strasbourg, France) for providing CABYV infectious plasmid pBin35SCA-WT. This work was supported by the National Key Basic Research Program of China (2006CB101903), the Natural Science Foundation of Beijing, China (6082006) and the Foundation of State Key Laboratory for Agrobiotechnology (2009 SKLAB05-7).

References

Baumberger, N., Tsai, C.H., Lie, M., Havecker, E., Baulcombe, D.C., 2007. The polerovirus silencing suppressor P0 targets ARGONAUTE proteins for degradation. Curr. Biol. 17, 1609–1614.
Bortolamiol, D., Pazhouhandeh, M., Marrocco, K., Genschik, P., Ziegler-Graff, V., 2007. The polerovirus F box protein P0 targets ARGONAUTE1 to suppress RNA silencing. Curr. Biol. 17, 1615–1621.
Cardozo, T., Pagano, M., 2004. The SCF ubiquitin ligase: insights into a molecular machine. Nat. Rev. Mol. Cell Biol. 5, 739–751.
Csorba, T., Lózsa, R., Hutvágner, G., Burgyán, J., 2010. Polerovirus protein P0 prevents the assembly of small RNA-containing RISC complexes and leads to degradation of ARGONAUTE1. Plant J. 62, 463–472.

Hamilton, A.J., Baulcombe, D.C., 1999. A novel species of small antisense RNA in post-transcriptional gene silencing. Science 286, 950–952.
Han, C., 2008. Molecular characterization of a Chinese sugar beet-infecting isolate of *Beet western yellows virus*. Phytopathology 98, S65.
Hofgen, R., Willmitzer, L., 1988. Storage of competent cells for Agrobacterium tumefaciens transformation. Nucleic Acids Res. 16, 9877-9877.
Kozlowska-Makulska, A., Guilley, H., Szyndel, M., Beuve, M., Lemaire, O., Herrbach, E., Bouzoubaa, S., 2009. The P0 proteins of European beet-infecting poleroviruses display variable silencing suppression activity. J. Gen. Virol. 91, 1082–1091.
Ma, B., Nussinov, R., 2007. Trp/Met/Phe hot spots in protein–protein interactions: potential targets in drug design. Curr. Top. Med. Chem. 7, 999–1005.
Ma, B., Elkayam, T., Wolfson, H., Nussinov, R., 2003. Protein–protein interactions: structurally conserved residues distinguish between binding sites and exposed protein surfaces. Proc. Natl. Acad. Sci. U. S. A. 100, 5772–5777.
Mangwende, T., Wang, M.L., Borth, W., Hu, J., Moore, P.H., Mirkov, T.E., Albert, H.H., 2009. The P0 gene of Sugarcane yellow leaf virus encodes an RNA silencing suppressor with unique activities. Virology 384, 38–50.
Pazhouhandeh, M., Dieterle, M., Marrocco, K., Lechner, E., Berry, B., Brault, V., Hemmer, O., Kretsch, T., Richards, K.E., Genschik, P., 2006. F-box-like domain in the polerovirus protein P0 is required for silencing suppressor function. Proc. Natl. Acad. Sci. U. S. A. 103, 1994–1999.
Pfeffer, S., Dunoyer, P., Heim, F., Richards, K.E., Jonard, G., Ziegler-Graff, V., 2002. P0 of beet western yellows virus is a suppressor of posttranscriptional gene silencing. J. Gen. Virol. 76, 6815–6824.
Ruiz, M.T., Voinnet, O., Baulcombe, D.C., 1998. Initiation and maintenance of virus-induced gene silencing. Plant Cell 10, 937–946.
Voinnet, O., Vain, P., Angell, S., Baulcombe, D.C., 1998. Systemic spread of sequence-specific transgene RNA degradation is initiated by localised introduction of ectopic promoterless DNA. Cell 95, 177–187.
Wallace, L.A., Burke, J., Dirr, H.W., 2000. Domain–domain interface packing at conserved Trp-20 in class α glutathione transferase impacts on protein stability. Biochim. Biophys. Acta Proteins Proteomics 1478, 325–332.
Welfle, H., Missel Witz, R., Welfle, K., Schindelin, H., Scholtz, A.S., Heinemann, U., 1993. Conformations and conformational changes of four Phe→ Trp variants of the DNA-binding histone-like protein, HBsu, from Bacillus subtilis studied by circular dichroism and fluorescence spectroscopy. Eur. J. Chem. 217, 849–856.
Xiang, H., Shang, Q., Han, C., Li, D., Yu, J., 2008. Complete sequence analysis reveals two distinct poleroviruses infecting cucurbits in China. Arch. Virol. 153, 1155–1160.
Xiang, H., Shang, Q., Han, C., Li, D., Yu, J., 2009. Detection of Turnip yellows virus in eight cruciferous crops in Mainland China. Phytopathology 99, S144.
Zhou, G.H., Li, J.G., Xu, D.L., Shen, W.K., Deng, H.H., 2006. Occurrence of *Sugarcane yellow leaf virus* in South China and its transmission by the sugarcane-colonizing aphid, *Ceratovacuna lanigera*. Sci. Agric. Sin. 39, 2023–2027.